

Holocene hydrological changes in Europe and the role of the North Atlantic ocean circulation from a speleothem perspective

Attila Demény^{a,*}, Zoltán Kern^a, István Gábor Hatvani^a, Csaba Torma^b, Dániel Topál^a,
Silvia Frisia^c, Szabolcs Leél-Óssy^d, György Czuppon^a, Gergely Surányi^{e,f}

^a Institute for Geological and Geochemical Research, Research Centre for Astronomy and Earth Sciences, Budaörsi út 45, Budapest, H-1112, Hungary

^b Department of Meteorology, Eötvös Loránd University, Pázmány Péter Sétány. 1/a, Budapest, H-1117, Hungary

^c University of Newcastle Australia, Earth Sciences, CHALLAGAN, Australia

^d Department of Physical and Applied Geology, Eötvös Loránd University, Pázmány Péter Sétány. 1/C, Budapest, H-1117, Hungary

^e MTA-ELTE Geological, Geophysical and Space Sciences Research Group, 1117, Budapest, Pázmány Péter s. 1/c, Hungary

^f Institute for Nuclear Research, Bem Tér 18/c, Debrecen, H-4026, Hungary

ARTICLE INFO

Keywords:

European and mediterranean regions
Speleothems
Stable isotope compositions
Principal component analysis
Holocene hydroclimate
Ocean circulations

ABSTRACT

Societal concerns about future hydroclimate changes urge a thorough understanding of the governing processes. Here, an analysis of Middle and Late Holocene speleothem-based hydroclimate reconstructions and paleoclimate model simulations reveals sub-millennial fluctuations in the spatiotemporal variability of precipitation in the European and Mediterranean regions, that complements previous dendrochronological and pollen-based reconstructions with an improved temporal resolution. Although insolation forcing is the primary driver of Holocene hydroclimate changes in Europe on a multimillennial scale, the evaluation of the principal component analysis of speleothem records and correlations with sea surface temperature data indicates that North Atlantic ocean circulation played a significant role in the sub-millennial variation of continental moisture transport, with an increasing importance during the Late Holocene. The combined evaluation of speleothem-based data, climate simulations and sea surface temperature records therefore advances our understanding of the governing processes of Holocene hydroclimate changes in the European and Mediterranean regions.

1. Introduction

Instrumental observations and modelling studies have shown that, in addition to temperature variations, humidity changes can also exert a significant force on our society (e.g., Hegerl et al., 2015; Mazurczyk et al., 2018). The evaluation of potential influences that may be expected under changing climate conditions at a given location requires knowledge of how the studied region responded to similar changes in the past. Coupled changes in temperature and precipitation amount may have initiated or contributed to societal processes, like the emergence and fall of empires, mass migration, agricultural development or crisis, and famine (e.g., McMichael, 2012; Sharifi et al., 2015; Drake, 2017). The European and Mediterranean regions are among the best areas to study the relationship between climate and society, due to its high population density, rich history of civilizations, and ample historical and instrumental records. Moreover, the Mediterranean and Northeastern Europe are also considered to be potential climate change hotspots in the

future, based on regional mean changes of surface air temperature and precipitation, as well as their interannual variability, derived from global climate simulations (Giorgi, 2006).

Hydroclimate reconstructions in Europe are dominated by tree ring and lake sediment data, with an imbalance towards Northwestern Europe in the tree ring datasets (Edvardsson et al., 2016). To date, the European Pollen Database (EPD, Davis et al., 2003) likely offers the best spatiotemporal coverage to reconstruct European post-glacial climate, which was used to create maps of seasonal temperature and precipitation variations in the European and Mediterranean regions at millennial-scale intervals over the last 12 ka (Mauri et al., 2015). The pollen assemblages, however, usually reflect the response of vegetation to climate changes on a large geographic scale, which has a centennial time lag with respect to the actual onset of climate variability. This time lag appears to affect paleoclimate reconstructions at a finer temporal resolution, but not an environmental reconstruction at millennial steps (Mauri et al., 2015). Combined application of climate models and

* Corresponding author.

E-mail address: demeny@geochem.hu (A. Demény).

<https://doi.org/10.1016/j.quaint.2020.10.061>

Received 22 May 2020; Received in revised form 22 October 2020; Accepted 25 October 2020

Available online 28 October 2020

1040-6182/© 2020 The Author(s).

Published by Elsevier Ltd.

This is an open access article under the CC BY-NC-ND license

(<http://creativecommons.org/licenses/by-nc-nd/4.0/>).

pollen-based environmental reconstructions are generally available for only a few selected periods, due to the computational limits and the issue of vegetation response lag. For example, a comparison of pollen-based precipitation reconstructions and results of global climate model simulations suggests that during the Middle Holocene, both the Middle and Eastern Mediterranean regions were characterized by humid conditions, whereas the Northern Mediterranean was relatively arid; the opposite occurred during the Late Holocene (Peyron et al., 2017). The temporal resolutions of these vegetation proxies and climate model studies do not allow for the investigation of the transition processes between the two climate states. The detection of the rapid climate processes that affected Europe and the Mediterranean region requires the investigation of climate archives that respond to environmental changes at annual to decadal time scales, that can be precisely and accurately dated by radiometric methods or annual layer counting, and that can be sampled at high resolution to extract climate proxy data.

In the continental environment, speleothems (mainly carbonate formations in caves, e.g., stalagmites and flowstones) can fulfil these requirements, making them an excellent archive of past climate and environmental data, due to their chemical and physical properties that enable extraction of information on climatic and environmental changes (Fairchild and Baker, 2012). Speleothems form in caves, which are “conservative” environments protected from surface weathering and erosion, and, when fed through fractures in the carbonate host rock, they may respond rapidly (within days) to hydroclimate changes. Speleothems can be precisely dated by U-series methods and contain a wealth of climate and environmental proxy data that, due to good age constraint, can be correlated over an entire continent (e.g., McDermott, 2004; Dorale and Liu, 2009). Thus, speleothems are well-suited for investigating past climate change processes in Europe and the associated environmental responses at high temporal resolution, typically at a sub-millennial scale. For example, comparisons of stable oxygen isotope variability in European speleothems have been used to detect continental-scale influences of ocean current variations and shifts in the synoptic meteorological systems during the Holocene (McDermott et al., 2011; Deininger et al., 2017). Furthermore, annual variability in lamina thickness of European stalagmites from high latitude and/or elevation has highlighted that solar variability is one of the drivers of climate (mostly as a temperature effect) at a decadal to a secular scale (Proctor et al., 2002; Frisia et al., 2003). Speleothems also capture external climate forcing agents, such as volcanic eruptions, specifically those that have a global impact, and allow for the correlation of coeval perturbances in the system from the poles to the low latitudes (Frisia et al., 2005, 2008; Badertscher et al., 2014).

In the last decade, there were significant advances in speleothem science that have allowed for regional paleoclimate syntheses (e.g., Braun et al., 2019; Deininger et al., 2019; Kern et al., 2019; Oster et al., 2019; Zhang et al., 2019). The European and Mediterranean regions have high speleothem data density compared to other regions of the world, except for China (Comas-Bru et al., 2019). Thus, we imply that calcium carbonate speleothems are likely one of the most accurate archives of continental European climate variability. Speleothems contain interrelated climate proxies, such as their microscopic textures and geochemical data (Fairchild and Baker, 2012; Frisia et al., 2018). Historically, the most frequently reported calcium carbonate speleothem data are their stable carbon and oxygen isotope compositions (expressed as $\delta^{13}\text{C}$ and $\delta^{18}\text{O}$ values, respectively, see below). Local processes, like vegetation, soil activity, carbonate precipitation along the route of karstic water migration, host rock dissolution, and kinetic fractionation related to degassing (see Fairchild and Baker, 2012), may affect stable carbon isotope ratios. As a result, the majority of research has focused on variations of oxygen isotope ratios, which may provide information on temperature, precipitation amount, and moisture transport directions (i.e., tracks) (Lachniet, 2009). Consequently, stable carbon and oxygen isotope compositions have been interpreted to reflect past hydroclimate variability at several European locations, particularly if they are

combined with independent paleohydrological proxy data (Fairchild and Baker, 2012). The independent palaeohydrological information may be extracted from the speleothems themselves (e.g., Mg and P contents, Treble et al., 2003) or from other archives, such as tree rings or lake sediments (e.g., Bolliet et al., 2016). As demonstrated in a comprehensive study on Mediterranean, Atlantic, and continental climate sites from Europe (Lellei-Kovács et al., 2016), soil respiration that supplies biogenic carbon to the groundwater and eventually to the drip water responds to temperature and humidity changes on an annual scale. Stable oxygen isotope compositions of meteoric and drip waters are dependent on precipitation amount, and this is characteristic of Mediterranean cave sites (e.g., Bar-Matthews et al., 2000; Bard et al., 2002; Drysdale et al., 2004; Zanchetta et al., 2007; 2014). The time lag between the surface signal of environmental change and the speleothem response is generally several weeks (e.g., Fohlmeister et al., 2010) or months (e.g., van Rampelbergh et al., 2014), but it depends on water migration rate and rock thickness above the cave. Thus, the time lag of a speleothem composition’s response to environmental change is negligible compared to the century-scale response of vegetation reflected by the pollen assemblages (see above).

The aim of the present study is to provide a compilation of speleothem-based hydroclimate records, which is urgently needed to complement tree ring and pollen-based reconstructions and, therefore, to advance our understanding of the processes that governed Holocene hydroclimate changes in the European and Mediterranean regions. We focus on hydroclimate conditions inferred in earlier studies from stable isotope and trace element compositions of European Holocene speleothems, along with paleoclimate model simulations. For this purpose, the spatial and temporal relationships between selected paleohumidity records are investigated in this paper by comparing their internal variabilities and by calculating correlation coefficients. Principal Component Analysis (PCA) is applied to ascertain if there is a shared variance in the speleothem based paleohydrological records. Finally, we present correlations between the PCA scores and North Atlantic sea surface temperature reconstructions and oceanographic data, to explore a potential connection between continental hydroclimate changes and oceanic conditions.

2. Data and methods

A total of 17 published speleothem-related records was gathered from the European and Mediterranean regions (spanning -8.8° W to 35.6° E and 32.9° N to 64.9° N; the list of sample locations is given in the Supplementary Material) that reflect paleohydrological changes based on independent evidence from previous studies. The selected records have appropriate age control and analytical resolution to allow for the investigation of sub-millennial variations in the Late Holocene. The records were either available in public datasets or were provided by the authors (MB-3, Milbach Cave, Austria – from Marc Luetscher; MAR_I, Skala Marion Cave, Greece – from David Psomiadis; CC26, Corchia Cave, Italy – from Eleonora Regattieri; BG composite record, Buraca Gloriosa Cave, Portugal – Diana Thatcher; North Atlantic sea surface temperature data of Eynaud et al., 2018 – from Frédérique Eynaud). The available records were selected so that their original age models had at least one radiometric age per each 1000 years, and that the datasets show sufficient sampling resolution (<50 years per data) to investigate centennial changes (see Supplementary Material). The dataset consists of stable carbon and oxygen isotope ratios, except the precipitation amounts in mm, which were inferred from Mg/Ca ratios of a stalagmite from the Cloşani Cave, Romania (Warken et al., 2018), and the lamina thickness values from the Uamh an Tartair Cave, NW Scotland (Baker et al., 2015). Standard statistical methods were applied for data analyses, including calculations of interval means, Pearson and Spearman rank correlation coefficients, and Principal Component Analysis. Further details are given in the Supplementary Material.

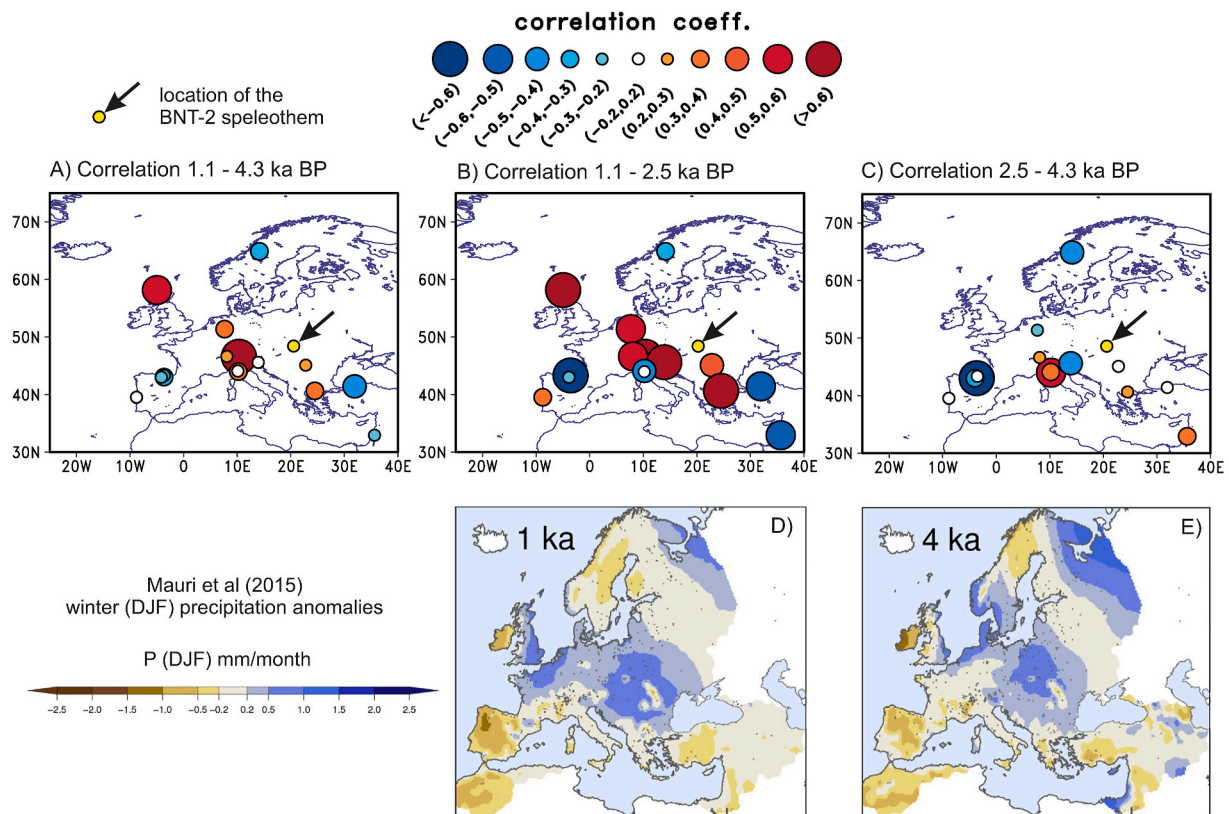


Fig. 1. Spatial coherence in reconstructed European hydroclimate anomalies estimated from palynological and speleothem-derived proxies. A, B, C: Spatial distribution of the coefficients of Spearman rank correlation between the BNT-2 $\delta^{13}\text{C}$ data and paleohydrological records for selected periods. D, E: Maps of winter precipitation anomalies (Mauri et al., 2015) for 1 and 4 ka BP, respectively. The location of the reference record (BNT-2, Demény et al., 2019) is shown by the arrow and the yellow circle. Sources of data: Baker et al. (2015), Boch and Spötl (2011), Cheng et al. (2015), Demény et al. (2019), Domínguez-Villar et al. (2017), Fleitmann et al. (2009), Fohlmeister et al. (2012), Frisia et al. (2005), Luetscher et al. (2011), Martín-Chivelet et al. (2011), Psomiadis et al. (2018), Regattieri et al. (2014), Smith et al. (2016), Sundqvist et al. (2010), Thatcher et al. (2020), Warken et al. (2018), Zanchetta et al. (2016). Description of locations are given in the Supplementary Material. (For interpretation of the references to color in this figure legend, the reader is referred to the Web version of this article.)

3. Results

3.1. Spatial patterns and relationships of speleothem compositions

After reducing the data to 200-year averages, Spearman rank correlation coefficients were calculated between the selected speleothem records and a reference dataset. The BNT-2 $\delta^{13}\text{C}$ record (Demény et al., 2019) was chosen as the reference record in the correlation calculations, because it is in a central position close to the maritime-continent climate boundary investigated by Breitenbach et al. (2019). The correlation coefficients were plotted to visualize their spatial distribution and to detect potential systematic patterns (Fig. 1).

Spearman rank correlation coefficients were determined for the entire period of 4.3 to 1.1 ka BP (thousands of years Before Present, i.e., before 1950 CE), as well as for shorter periods of 4.3 to 2.5 ka BP and of 2.5 to 1.1 ka BP to test potential secular changes in the correlation pattern. The spatial correlation pattern for the 4.3 to 1.1 ka BP interval (Fig. 1A) resembles the large-scale pattern that is reconstructed in the map of winter precipitation anomalies, as inferred from pollen assemblages (Mauri et al., 2015) (Fig. 1D and E), which shows similar humidity conditions ranging from Eastern Europe to Wales, but contrasting behavior in Iberia and the Levant. Winter precipitation patterns were selected from the maps of Mauri et al. (2015), as drip waters in caves are generally affected by selective infiltration of cold season precipitation, due to evaporation in warm months, and in this way the speleothem-based patterns are comparable with the pollen-based maps. However, when the 4.3–1.1 ka BP period is further divided into 4.3–2.5 ka BP and 2.5–1.1 ka BP time slices, the patterns change slightly (Fig. 1B

and C). At 4 ka BP (Fig. 1E), the wet region is smaller and shifted northwards, compared to the scenario obtained for the 1 ka BP interval (Fig. 1D). Records from Central and Western Europe show less pronounced correlations with the BNT-2 $\delta^{13}\text{C}$ record for the 2.5–4.3 ka BP period (Fig. 1C) than for the 1.1–2.5 ka BP period (Fig. 1B). The pollen database suggests that the shoreline of the Levant was characterized by wet conditions at ~4 ka (Fig. 1E), and the stalagmite record for this region (Jeita Cave $\delta^{13}\text{C}$ record, Lebanon, Cheng et al., 2015) shows a slight positive correlation with the BNT-2 $\delta^{13}\text{C}$ data for the 4.3 to 2.5 ka BP period (Fig. 1C). The pollen-based paleohumidity reconstruction at 1ka BP shows that the wet zone shifted southward and became more pronounced in Central Europe and the northern part of Western Europe (Fig. 1D). As a result, the BNT-2 $\delta^{13}\text{C}$ record yielded stronger positive correlations along a SE-NW traverse from the Aegean Sea to the Scottish Highlands and across Central Europe, but emphasized negative correlations with the records of Iberia, and the Levant for the 2.5 to 1.1 ka BP period (Fig. 1B).

The correlation patterns of the speleothem-based European paleohumidity records resemble the pollen-based winter precipitation anomaly maps; however, the current availability of data required for the correlation calculations precluded an evaluation of secular changes at higher resolution. Furthermore, water-balance changes at individual locations could not be assessed quantitatively from the correlation patterns. Thus, internal variabilities of each record were quantified relative to the records' mean values in the 2–3 ka BP period (representing the common overlapping period), which calculation yielded % changes in the relative precipitation amount, compared to the common period ("speleothem internal variability": SIV). The procedure,

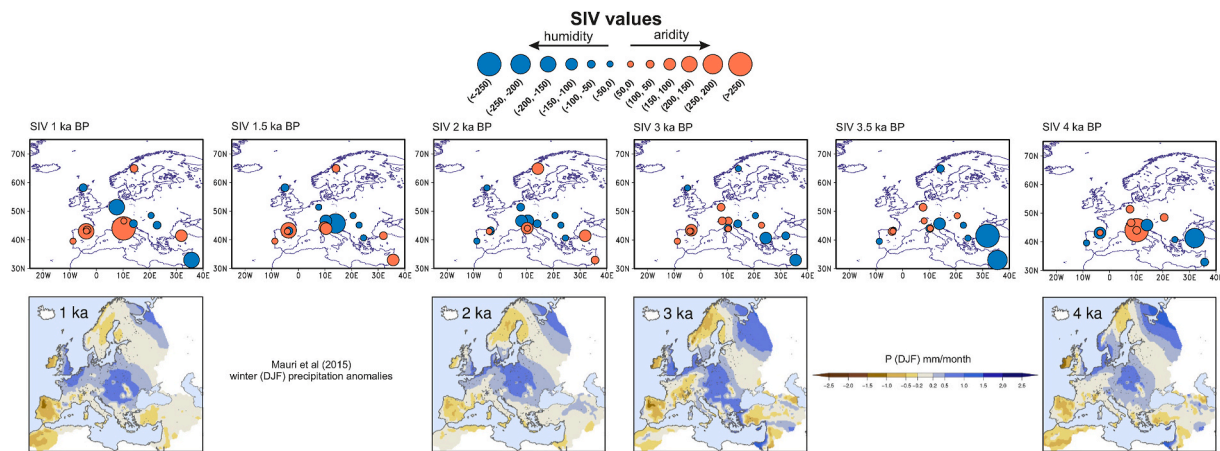


Fig. 2. Upper panel: Spatial structure of hydroclimate changes over the past 4000 years in Europe, represented by speleothem internal variability (SIV) maps with 500-year time slices. SIV values are compared to the 2–3 ka BP averages, thus, the 2.5 ka BP pattern is not shown. Lower panel: Winter precipitation anomaly maps of Mauri et al. (2015). See Supplementary Material for speleothem locations.

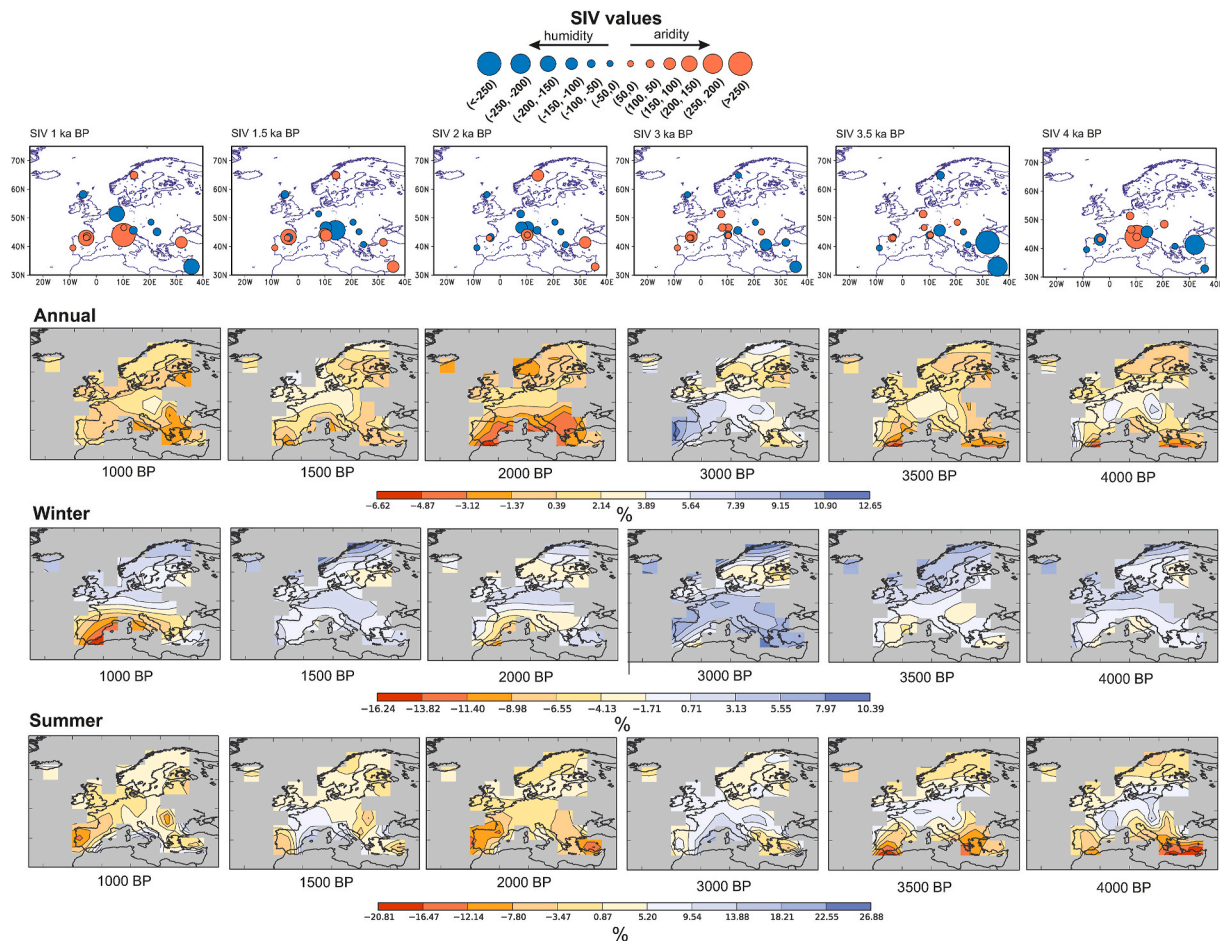


Fig. 3. Speleothem internal variability maps (see Fig. 2) and annual and seasonal precipitation amount changes, relative to 2.5 ka BP. Precipitation maps were obtained from PaleoView (Fordham et al., 2017).

described in detail in the Supplementary Material, yielded data with 500-year time steps that were plotted together with pollen-based winter precipitation anomaly maps (Fig. 2).

The SIV maps and the pollen-based winter precipitation anomalies exhibit similar spatial patterns (Fig. 2). Compared to the 4 ka BP map, both datasets suggest the existence of a NW-SE trending humidity belt at 3 ka, with wetter conditions (relative to the 2–3 ka BP common period)

in the Levant, the Balkan Peninsula, the Carpathian Region, the Scottish Highlands and Scandinavia. In contrast, central Western Europe and Iberia experienced increased aridity, relative to the 2–3 ka BP common period. At 2 ka BP, this situation reversed, with moist conditions in Central Europe and increasing aridity in the Levant. The number of records spanning the last 1 ka BP decreased, but they still indicate drier conditions in Iberia, the northern part of the Apennine Peninsula,

Anatolia, and the western part of Scandinavia.

3.2. Comparison with climate model data

Comparison of climate model data with the SIV maps can further elucidate governing processes of spatial hydroclimate variations across Europe during the Late Holocene, both at seasonal and annual time scales. Climate model data were assessed in the PaleoView program, which uses the product of the TRaCE21ka experiment (Fordham et al., 2017). The TRaCE21ka experiment is based on the output of the Community Climate System Model ver. 3 (CCSM3; Collins et al., 2006; Otto-Bliesner et al., 2006; Yeager et al., 2006) and covers the period from 22 ka BP to the Present (1989 CE). Although the assessment of an ensemble of climate models would be ideal, such transient multimillennial paleoclimate model simulations remain unavailable (Otto-Bliesner et al., 2017).

Changes in annual, winter (DJF), and summer (JJA) averages of precipitation amounts were computed relative to the period of 2.5 ka BP, with a 100 yr time window (the maximum interval in PaleoView) (Fig. 3). The SIV calculation interval was longer for the speleothems (500 years), and the reference period for the speleothems was 2.5 ± 0.5 ka BP, due to the lower data frequency for some periods and records. In contrast to the pollen humidity maps of Mauri et al. (2015), PaleoView maps allow for the investigation of temporal and spatial changes at the 500 yr resolution of the speleothem map series.

The results show that an expansion of less arid conditions (relative to the 2–3 ka BP period) appears at 3.5 ka BP in the speleothem map and at 3 ka BP in the climate model data (Fig. 3), but the relationships are more complex in other periods. However, close inspection of the maps reveals systematic changes. At 4 ka BP, the speleothem-based hydroclimate pattern primarily resembles the winter precipitation distribution, with the eastern Mediterranean being wet and northern Italy being relatively dry. The 3.5 ka BP and 4 ka BP humidity distribution patterns are similar, with slightly more arid conditions extending northward from the western Mediterranean, where the effect of summer precipitation appears to be stronger. On the west coast of Scandinavia, the effect of winter precipitation dominates until 3 ka BP. The distributions of precipitation change alter significantly after 3 ka BP. At 2 ka BP, Western and Central Europe follow the winter P change map, while in Western Scandinavia and the Eastern Mediterranean, the summer precipitation change appears to dominate and persist to 1.5 ka BP. At 1 ka BP, drier conditions generally prevailed, except in the Levant, where the speleothem record indicates wet conditions, similarly to the distribution of winter precipitation change.

These observations indicate that sub-millennial fluctuations in hydroclimate detected in speleothems are reflected in the independent climate model simulations, as well, and their comparison elucidates the effects of spatial and temporal changes in precipitation conditions during the Late Holocene.

3.3. Leading modes in speleothem-based hydroclimate records

The mechanisms and processes that controlled paleohydroclimate fluctuations across Europe can be investigated with Principal Component Analysis (PCA). PCA compresses the common linear variance of the chosen records into Principal Components (PCs) that can be compared to independent paleoclimate records and to the effects of potential climate drivers.

The first (PC1) and second (PC2) PCs are described and compared in the Supplementary Material. The PCs calculated for shorter periods (4.3–1.1 and 8.2 to 4.3 ka BP) reflect multicentennial-millennial fluctuations, whereas the PC1 data obtained for the 8.2 to 1.1 ka BP period indicate a long-term trend (Fig. S4). The PCs yielded for 6 or 9 speleothem records show a good agreement (Fig. S4), indicating that the number of selected records does not affect the results.

The PC1(9) data obtained for 9 records for the period of 4.3 to 1.1 ka

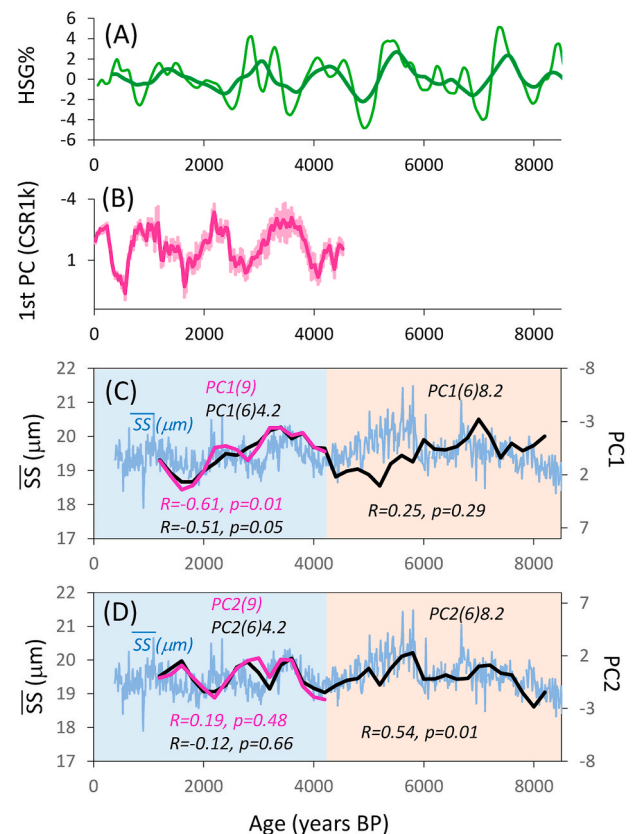


Fig. 4. (A) Composite hematite stained grains (HSG) % values of North Atlantic Ocean sediment cores (Bond et al., 2001), (B) leading mode of variability of 11 European speleothem $\delta^{18}\text{O}$ records (CSR1k, Deininger et al., 2017), (C) and (D) sortable silt (SS) mean size data of the GS06-144 08 GC core (Mjell et al., 2015) and speleothem-based PC data of this study. PC1(9) and PC2(9) – PC1 and PC2 obtained for 9 records for the period of 4.3 to 1.1 ka BP (pink lines); PC1(6) and PC2(6) – PC1 and PC2 obtained for 9 records (black lines); 4.2 marks the period of 4.3 to 1.1 ka BP; 8.2 marks the period of 8.2 to 4.3 ka BP. Correlation coefficients between the SS mean data and the speleothem PCs (color codes as for PCs) for different age periods (8.2–4.3 and 4.3 to 1.1 ka BP periods separated) are also shown. (For interpretation of the references to color in this figure legend, the reader is referred to the Web version of this article.)

BP (see Supplementary Material) are plotted together with the 1st PC (CSR1k) dataset from Deininger et al. (2017) (Fig. 4B), which was obtained from the principal component analysis of $\delta^{18}\text{O}$ records of 11 European speleothems and showed firm relationships with North Atlantic ocean current strength (Deininger et al., 2017). The PC1(9) and the CSR1k records display a significant linear correlation ($r = 0.64$, $p < 0.01$; using 200-year averages for both records).

The PC1(9) data were also compared to sedimentary proxies for oceanic circulation intensity of the North Atlantic sub-polar gyre (Mjell et al., 2015) and Arctic sea-ice dynamics (Bond et al., 2001) (Fig. 4A), with the assumption that European speleothem derived hydroclimate signals respond to North Atlantic climate influences (Deininger et al., 2017). The result suggests that European paleohydrological conditions are also closely related to climate processes that have been operating in the North Atlantic over the past 4000 years. This hypothesis is further investigated in the following section.

3.4. Speleothem compositions and North Atlantic sea surface temperatures

Sea surface temperature (SST) provides essential information about the boundary conditions of the climate system, thus, reconstructed SST records in the North Atlantic realm were selected from recent

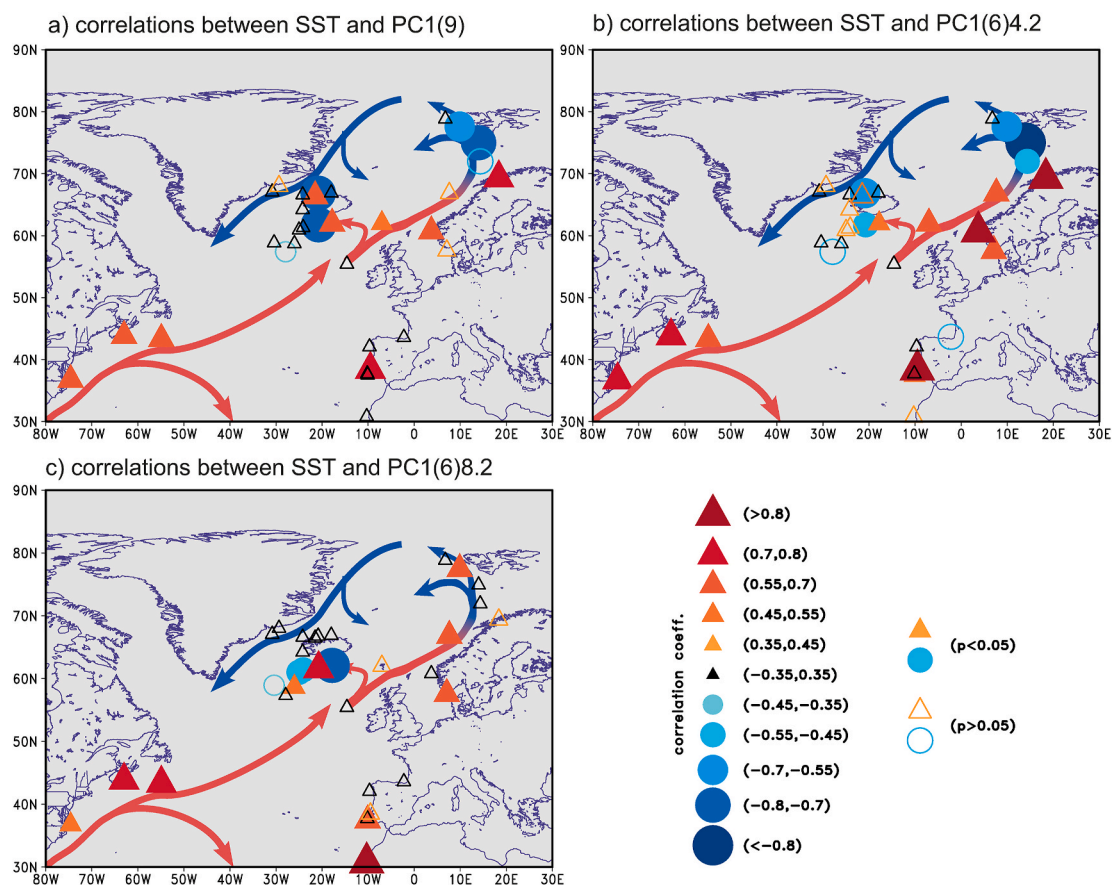


Fig. 5. Correlation coefficients between sea surface temperature records (Sundqvist et al., 2014; Eynaud et al., 2018) and PC1 data. PC1(9): 9 speleothem records, 1.1–4.3 ka BP; PC1(6)4.2: 6 speleothem records, 1.1–4.3 ka BP; PC1(6)8.2: 6 speleothem records, 4.3–8.2 ka BP (see Supplementary Material). Tracks of warm (red) and cold (blue) ocean currents are schematically shown. (For interpretation of the references to color in this figure legend, the reader is referred to the Web version of this article.)

compilations (Sundqvist et al., 2014; Eynaud et al., 2018) and were correlated with the leading principal component (PC1) time series of speleothem records calculated for the 4.3 to 1.1 ka BP and 8.2 to 4.3 ka BP periods (see Supplementary Material). The PC2 records did not yield statistically significant correlations. It should be noted that, stemming from the mathematical background of the Principal Component Analysis, it is not the sign of the correlations that is important, but rather the variability and relationships within the database. Mapping the SST-PC1 correlation coefficients across the North Atlantic realm (Fig. 5) highlights clusters of positive and negative correlations between the PC1 and SST reconstructions. Positive correlations are consistently found along warm ocean currents, while opposite PC1-SST relationships appear around the cold East Greenland Current for all the PC1 calculations (9 vs. 6 records, younger vs. older periods).

The long-term trend (Fig. S4) in the PC1(6)T (leading mode extracted from 6 records for the entire 8.2 to 1.1 ka BP period) data was also detected in the SST records at different locations in the North Atlantic, as exemplified by three SST reconstructions from the coastal regions of Scandinavia (Malangen fjord, Norway), NW Iceland (MD99-2266), and Iberia (MD01-2244) (Fig. 6).

4. Discussion

The spatiotemporal changes of speleothem-based hydroclimate conditions, as well as their relationships with climate model data, North Atlantic SST records, and ocean current pathways (Fig. 6) collectively suggest that the Atlantic Meridional Overturning Circulation (AMOC) system had a strong effect on the Middle and Late Holocene

hydroclimate fluctuations in the European and Mediterranean regions. Moisture transport processes and precipitation distribution in Europe are determined by the interplay of solar forcing, the North Atlantic Oscillation (NAO), the Atlantic Multidecadal Oscillation (AMO), North Atlantic storms, and cyclonic activity (Mojtahid et al., 2019; Goslin et al., 2019), resulting in pronounced spatial differences in precipitation distribution across the North Atlantic domain (Auger et al., 2019). Using major storm track systems, Dong et al. (2013) detected two primary precipitation distribution regimes: the wet Northern Europe and the dry Southern Europe. Ummenhofer et al. (2017) discerned five major precipitation distribution regimes (patterns A to E) within Europe, with a complex pattern of wet and dry regions, using cluster analysis of observational data and reanalysis products (e.g., sea level pressure, air and sea surface temperatures, winds, geopotential height, and precipitation amount, gathered from various databases). Although the present-day regimes of Ummenhofer et al. (2017) are different to the Holocene patterns established by Mauri et al. (2015), pattern B of Ummenhofer et al. (2017) is similar to the 2 ka BP speleothem-based hydroclimate distribution. These observations and models correspond to recent processes and conditions, it is therefore important to compare them to long-term Holocene changes.

The observed temporal changes and Principal Component Analysis of hydroclimate-sensitive speleothem data revealed further linear relationships. The long-term trends of North Atlantic SST records, speleothem-based PC values, and relative changes in modelled precipitation amount averaged for Europe all show good correspondence with orbitally driven June insolation (Fig. 6). This supports the widely accepted notion that the primary governing factor of multimillennial

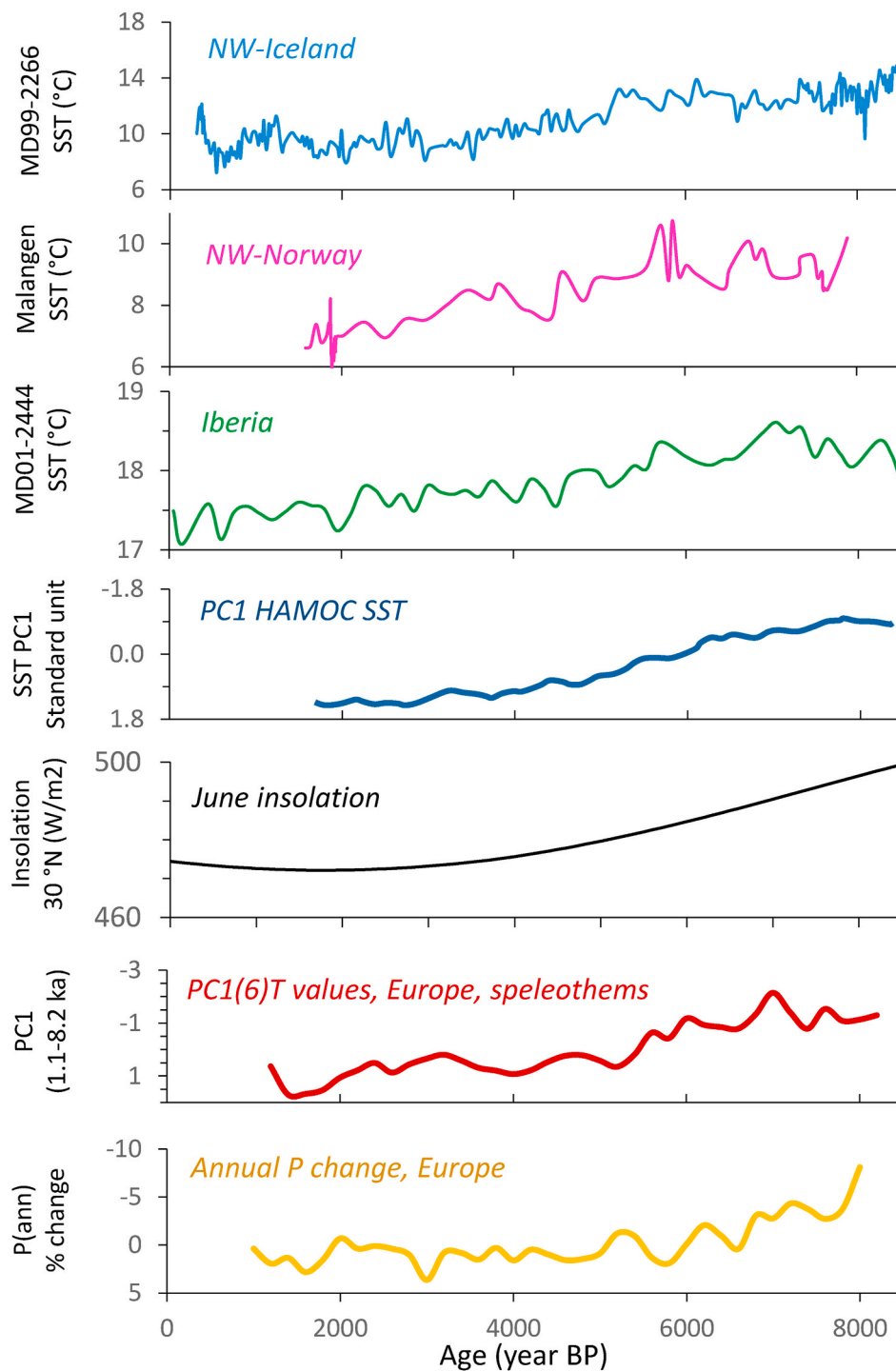


Fig. 6. Comparison of PC1(6)T data obtained for 6 speleothem records for the 8.2 to 1.1 ka BP period and selected sea surface temperature (SST), insolation values, and modelled changes in annual precipitation amount. SST records: MD99-2266 - Moossen et al. (2015); Malangen fjord - Sundquist et al. (2014); MD01-2444 - Martrat et al. (2007), Hodell et al. (2013). PC1 HAMOC record: Ayache et al. (2018). Insolation data for June for 30° N: Laskar et al. (2004). P(ann): Change in annual mean precipitation amount relative to 2.5 ka BP, as simulated by CCSM3 in TRaCE21ka experiment, averaged for “Europe” domain in Paleoview (Fordham et al., 2017).

shifts in ocean surface temperature and moisture transport is orbitally forced insolation variation. However, detailed evaluation of fluctuations in speleothem-based PC records and paleoceanographic data can detect matching patterns at the sub-millennial scale, as well. Deininger et al. (2017) showed that North Atlantic wind stress, which modulates the strength of the AMOC, is the mechanism behind the common component extracted from the oxygen isotope records of 11 Europe speleothems. The PC1 values of this study and the proxy of North Atlantic ocean current strength (mean sortable silt grain size, SS mean, Mjell et al., 2015) are well-correlated between 4.3 and 1.1 ka BP, but they appear to be uncorrelated before 4.3 ka (Fig. 4). In contrast to PC1 values, the PC2 data show good correlation with the SS mean values before 4.3 ka BP

and poor correlation after 4.3 ka BP. These observations suggest that the relationships between ocean currents and the European moisture transport that determined the speleothem compositions changed between 4 and 5 ka BP. Accordingly, our findings imply that Late Holocene humidity changes in Europe may have been affected by changes in North Atlantic SST, which were a complex response to changes in irradiance.

Similar conclusions about humidity changes and moisture transport processes around the Middle to Late Holocene transition were drawn in previous studies. Speleothem data from the Atlas Mts (Wintimdouine Cave, Morocco, Sha et al., 2019). and Western Iberia (Buraca Gloriosa Cave, Portugal, Thatcher et al., 2020) indicate increasingly drier conditions from ~4 ka BP, and they have been interpreted to reflect

southerly movement of the Intertropical Convergence Zone (ITCZ). Consequently, AMOC strength and moisture transport trajectories were also affected. The temporally changing relationships between speleothem-based PCs, SST values, and ocean current strength indicate that, although summer insolation was the dominant factor in Middle and Late Holocene moisture distribution for the European and Mediterranean regions, the role of North Atlantic ocean currents significantly increased after ~4 ka BP. As the ITCZ shifted southward, the role of moisture transport from the North Atlantic Ocean region became stronger in the Late Holocene.

5. Conclusions

Although stable isotope compositions of speleothems depend on several external and internal processes affecting the deposition of cave carbonates, in some cases, carbon and oxygen isotope values may reflect dominantly paleo-humidity conditions. Prompted by previous observations of close relationships between $\delta^{13}\text{C}$ values of a flowstone occurrence in East-Central Europe (the BNT-2 record, Demény et al., 2019), as well as by European paleo-hydrological proxy records, speleothem records reflecting variations in precipitation amount were correlated with the BNT-2 record. The spatial distributions of correlation relationships, as well as the sign and degree of internal isotope variation as a measure of humidity changes, mirror independent precipitation anomaly maps. Comparison with precipitation changes mapped in climate model simulations revealed complex relationships with spatiotemporal variations of seasonal precipitation distributions. The findings support the hypothesis that speleothem records provide reliable reconstructions of continental-scale paleo-humidity patterns. Principal Component Analysis of speleothem records was used to detect the common component behind the stable isotope ratio variability in the speleothem record. The temporal evolution of the 1st PC, deduced from speleothem data, was found to correlate well with North Atlantic sea surface temperature data, indicating that ocean current strength played a major role in moisture transport to the European continent throughout most of the Holocene.

Declaration of competing interest

The authors declare that they have no known competing financial interests or personal relationships that could have appeared to influence the work reported in this paper.

Acknowledgments

The study was financially supported by the National Research, Development and Innovation Office, Hungary (OTKA 101664 and PD 121387) and the Hungarian Academy of Sciences (NANOMIN project, KEP-8/2018; János Bolyai Research Scholarship to Csaba Torma; guest scientist invitation to Silvia Frisia). Speleothem and sea surface temperature data were gathered from the NOAA Paleoclimatology Database, or were generously provided by Frédérique Eynaud, Marc Luetscher, David Psomiadis, Eleonora Regattieri, and Diana Thatcher, whose help is gratefully acknowledged. Thank you to Ariana Gugora for editing the English of the manuscript.

Appendix A. Supplementary data

Supplementary data to this article can be found online at <https://doi.org/10.1016/j.quaint.2020.10.061>.

Author contributions

AD designed the research work and compiled the manuscript. ZK and SF participated in the interpretation and writing of the manuscript. IGH performed the statistical analyses. CsT gathered climate model data and contributed climate model interpretations. DT aided in the

interpretation of North Atlantic climate relationships. SzL, GyCz, and GS participated in speleothem collection, isotope analyses, and interpretation.

References

- Auger, J.D., Mayewski, P.A., Maasch, K.A., Schuenemann, K.C., Carleton, A.M., Birkel, S.D., Saros, J.E., 2019. 2000 years of North Atlantic-Arctic climate. *Quat. Sci. Rev.* 216, 1–17.
- Ayache, M., Swingedouw, D., Mary, Y., Eynaud, F., Colin, C., 2018. Multi-centennial variability of the AMOC over the Holocene: a new reconstruction based on multiple proxy-derived SST records. *Global Planet. Change* 170, 172–189.
- Badertscher, S., Borsato, A., Frisia, S., Cheng, H., Edwards, R.L., Tüysüz, O., Fleitmann, D., 2014. Speleothems as sensitive recorders of volcanic eruptions – the Bronze Age Minoan eruption recorded in a stalagmite from Turkey. *Earth Planet Sci. Lett.* 392, 58–66.
- Baker, A.C., Hellstrom, J., Kelly, B.F.J., Mariethoz, G., Trouet, V., 2015. A composite annual-resolution stalagmite record of North Atlantic climate over the last three millennia. *Sci. Rep.* 5, 10307.
- Bard, E., Delaygue, G., Rostek, F., Antonioli, F., Silenzi, S., Schrag, D., 2002. Hydrological conditions in the western Mediterranean basin during the deposition of Sapropel 6 (ca. 175 kyr). *Earth Planet Sci. Lett.* 202, 481–494.
- Bar-Matthews, M., Ayalon, A., Kaufman, A., 2000. Timing and hydrological conditions of Sapropel events in the Eastern Mediterranean, as evident from speleothems, Soreq cave, Israel. *Chem. Geol.* 169, 145–156.
- Boch, R., Spötl, C., 2011. Reconstructing palaeoprecipitation from an active cave flowstone. *J. Quat. Sci.* 26, 675–687.
- Bolliet, T., Brockmann, P., Masson-Delmotte, V., Bassinet, F., Daux, V., Genty, D., Landais, A., Lavrieux, M., Michel, E., Ortega, P., Risi, C., Roche, D.M., Vimeux, F., Waelbroeck, C., 2016. Water and carbon stable isotope records from natural archives: a new database and interactive online platform for data browsing, visualizing and downloading. *Clim. Past* 12, 1693–1719.
- Bond, G., Kromer, B., Beer, J., Muscheler, R., Evans, M., Showers, W., Hoffmann, S., Lotti-Bond, R., Hajdas, I., Bonani, G., 2001. Persistent solar influence on North Atlantic climate during the Holocene. *Science* 294, 2130–2136.
- Braun, K., Nehme, C., Pickering, R., Rogerson, M., Scroton, N., 2019. A window into Africa's past hydroclimates: the SISAL v1 database contribution. *Quaternary* 2–4.
- Breitenbach, S.F.M., Plessen, B., Waltgenbach, S., Tjallingii, R., Leonhardt, J., Jochum, K.P., Meyer, H., Goswami, B., Marwan, N., Scholz, D., 2019. Holocene interaction of maritime and continental climate in Central Europe: new speleothem evidence from Central Germany. *Global Planet. Change* 176, 144–161.
- Cheng, H., Sinha, A., Verheyden, S., Nader, F.H., Li, X.L., Zhang, P.Z., Yin, J.J., Yi, L., Peng, Y.B., Rao, Z.G., Ning, Y.F., Edwards, R.L., 2015. The climate variability in northern Levant over the past 20,000 years. *Geophys. Res. Lett.* 42, 8641–8650.
- Collins, W.D., Bitz, C.M., Blackmon, M., Bonan, G.B., Bretherton, C.S., Carton, J.A., Chang, P., Doney, S., Hack, J.J., Henderson, T., Kiehl, J.T., Large, W.G., McKenna, D., Santer, B.D., Smith, R., 2006. The community climate system model version 3 (CCSM3). *J. Clim.* 19, 2122–2143.
- Comas-Bru, L., Harrison, S.P., Werner, M., Rehfeld, K., Scroton, N., Veiga-Pires, C., SISAL working group members, 2019. Evaluating model outputs using integrated global speleothem records of climate change since the last glacial. *Clim. Past* (in press).
- Davis, B.A.S., Brewer, S., Stevenson, A.C., Guiot, J., 2003. The temperature of Europe during the Holocene reconstructed from pollen data. *Quat. Sci. Rev.* 22, 1701–1716.
- Deininger, M., McDermott, F., Mudelsee, M., Werner, M., Frank, N., Mangini, A., 2017. Coherency of late Holocene European speleothem $\delta^{18}\text{O}$ records linked to North Atlantic Ocean circulation. *Clim. Dynam.* 49, 595–618.
- Deininger, M., Ward, B.M., Novello, V.F., Cruz, F.W., 2019. Late quaternary variations in the south American monsoon system as inferred by speleothems – new perspectives using the SISAL database. *Quaternary* 2–6.
- Demény, A., Kern, Z., Németh, A., Frisia, S., Hatvani, I.G., Czuppon, Gy, Leél-Óssy, Sz, Molnár, M., Óvári, M., Surányi, G., Gilli, A., Wu, Ch-Ch, Shen, Ch-Ch, 2019. North Atlantic influences on climate conditions in East-Central Europe in the late Holocene reflected by flowstone compositions. *Quat. Int.* 512, 99–112.
- Domínguez-Villar, D., Wang, X., Krklec, K., Cheng, H., Edwards, R.L., 2017. The control of the tropical North Atlantic on Holocene millennial climate oscillations. *Geology* 45, 303–306.
- Dong, B., Sutton, R.T., Woolings, T., Hodges, K., 2013. Variability of the North Atlantic summer storm track: mechanisms and impacts on European climate. *Environ. Res. Lett.* 8, 034037.
- Dorale, J.A., Liu, Z., 2009. Limitations of Hendy test criteria in judging the paleoclimatic suitability of speleothems and the need for replication. *J. Caves Karst Stud.* 71, 73–80.
- Drake, B.L., 2017. Changes in North Atlantic oscillation drove population migrations and the collapse of the western roman empire. *Sci. Rep.* 7, 1227.
- Drysdale, R.N., Zanchetta, G., Hellstrom, J.C., Fallick, A.E., Zhao, J.-x., Isola, I., Bruschi, G., 2004. Palaeoclimatic implications of the growth history and stable isotope ($\delta^{18}\text{O}$ and $\delta^{13}\text{C}$) geochemistry of a Middle to Late Pleistocene stalagmite from central-western Italy. *Earth Planet Sci. Lett.* 227, 215–229.
- Edvardsson, J., Stoffel, M., Corona, Ch, Bragazza, L., Leuschner, H.H., Chraman, D.J., Helama, S., 2016. Subfossil peatland trees as proxies for Holocene palaeohydrology and palaeoclimate. *Earth Sci. Rev.* 163, 118–140.
- Eynaud, F., Mary, Y., Zumaque, J., Wary, M., Gasparotto, M.C., Swingedouw, D., Colin, C., 2018. Compiling multiproxy quantitative hydrographic data from

- Holocene marine archives in the North Atlantic: a way to decipher oceanic and climatic dynamics and natural modes? *Global Planet. Change* 170, 48–61.
- Fairchild, I.J., Baker, A., 2012. *Speleothem Science: from Process to Past Environments*. Wiley-Blackwell, p. 450.
- Fleitsmann, D., Cheng, H., Badertscher, S., Edwards, R.L., Mudelsee, M., Gökür, O.M., Frankhauser, A., Pickering, R., Raible, C.C., Matter, A., Kramers, J., Tüysüz, O., 2009. Timing and climatic impact of Greenland interstadials recorded in stalagmites from northern Turkey. *Geophys. Res. Lett.* 36, L19707.
- Fohlmeister, J., Schröder-Ritzrau, A., Spötl, C., Frisia, S., Miorandi, R., Kromer, B., Mangini, A., 2010. The influences of hydrology on the radiogenic and stable carbon isotope composition of cave drip water, Grotta di Ernesto (Italy). *Radiocarbon* 52, 1529–1544.
- Fohlmeister, J., Schröder-Ritzrau, A., Scholz, D., Spötl, C., Riechelmann, D.F.C., Mudelsee, M., Wackerbarth, A., Gerdes, A., Riechelmann, S., Immenhauser, A., Richter, D.K., Mangini, A., 2012. Bunker Cave stalagmites: an archive for central European Holocene climate variability. *Clim. Past* 8, 1751–1764.
- Fordham, D.A., Saltré, F., Haythorne, S., Wigley, T.M.L., Otto-Bliesner, B.L., Chan, K.C., Brook, B.W., 2017. PaleoView: a tool for generating continuous climate projections spanning the last 21 000 years at regional and global scales. *Ecography* 40, 1348–1358.
- Frisia, S., Borsato, A., Preto, N., McDermott, F., 2003. Late Holocene annual growth in three Alpine stalagmites records the influence of solar activity and the North Atlantic Oscillation on winter climate. *Earth Planet Sci. Lett.* 216, 411–424.
- Frisia, S., Borsato, A., Spötl, C., Villa, I.M., Cucchi, F., 2005. Climate variability in the SE Alps of Italy over the past 17 000 years reconstructed from a stalagmite record. *Boreas* 34, 445–455.
- Frisia, S., Borsato, A., Susini, J., 2008. Synchrotron radiation applications to past volcanism archived in speleothems: an overview. *J. Volcanol. Geoth. Res.* 177, 96–100.
- Frisia, S., Borsato, A., Hellstrom, J., 2018. High spatial resolution investigation of nucleation, growth and early diagenesis in speleothems as exemplar for sedimentary carbonates. *Earth Sci. Rev.* 178, 68–91.
- Giorgi, F., 2006. Climate change hot-spots. *Geophys. Res. Lett.* 33 (8).
- Goslin, J., Galka, M., Sander, L., Fruergaard, M., Monkenbusch, J., Thibault, N., Clemmensen, L.B., 2019. Decadal variability of north-eastern Atlantic storminess at the mid-Holocene: new inferences from a record of wind-blown sand, western Denmark. *Global Planet. Change* 180, 16–32.
- Hegerl, G.C., Black, Emily, Allan, Richard P., Ingram, W.J., Polson, D., Trenberth, K.E., Chadwick, R.S., Arkin, P.A., Balan Sarojini, B., Becker, A., Dai, A., Durack, P.J., Easterling, D., Fowler, H.J., Kendon, E.J., Huffman, G.J., Liu, C., Marsh, Robert, New, M., Osborn, T.J., Skliris, Nikolaos, Stott, P.A., Vidale, P.-L., Wijffels, S.E., Wilcox, L.J., Willett, K.M., Zhang, X., 2015. Challenges in quantifying changes in the global water cycle. *Bull. Am. Meteorol. Soc.* 96, 1097–1115.
- Hodell, D., Crowhurst, S., Skinner, L., Tzedakis, P.C., Margari, V., Channell, J.E.T., Kamenov, G., Maclachlan, S., Rothwell, G., 2013. Response of Iberian Margin sediments to orbital and suborbital forcing over the past 420 ka. *Paleoceanography* 28, 185–199.
- Kern, Z., Demény, A., Persoiu, A., Hatvani, I.G., 2019. Speleothem records from the eastern part of Europe and Turkey – discussion on stable oxygen and carbon isotopes. *Quaternary* 2, Paper 31.
- Lachniet, M.S., 2009. Climatic and environmental controls on speleothem oxygen-isotope values. *Quat. Sci. Rev.* 28, 412–432.
- Laskar, J., Robutel, P., Joutel, F., Gastineau, M., Correia, A.C.M., Levrard, B., 2004. A long term numerical solution for the insolation quantities of the Earth. *Astron. Astrophys.* 428, 261–285.
- Lellei-Kovács, E., Botta-Dukát, Z., de Dato, G., Estiarte, M., Guidolotti, G., Kopitke, G.R., Kovács-Láng, E., Kröel-Dulay, Gy, Larsen, K.S., Peñuelas, J., Smith, A.R., Sowerby, A., Tietema, A., Schmidt, I.K., 2016. Temperature dependence of soil respiration modulated by thresholds in soil water availability across European shrubland ecosystems. *Ecosystems* 19, 1460–1477.
- Luetscher, M., Hoffmann, D.L., Frisia, S., Spötl, C., 2011. Holocene glacier history from alpine speleothems, Milchbach cave, Switzerland. *Earth Planet Sci. Lett.* 302, 95–106.
- Martín-Chivelet, J., Muñoz-García, M.B., Edwards, R.L., Turrero, M.J., Ortega, A.I., 2011. Land surface temperature changes in Northern Iberia since 4000 yr BP, based on $\delta^{13}\text{C}$ of speleothems. *Global Planet. Change* 77, 1–12.
- Martrat, B., Grimalt, J.O., Shackleton, N.J., de Abreu, L., Hutterli, M.A., Stocker, T.F., 2007. Four climate cycles of recurring deep and surface water destabilizations on the Iberian margin. *Science* 317, 502–507.
- Mauri, A., Davis, B.A.S., Collins, P.M., Kaplan, J.O., 2015. The climate of Europe during the Holocene: a gridded pollen-based reconstruction and its multi-proxy evaluation. *Quat. Sci. Rev.* 112, 109–127.
- Mazurczyk, T., Piekielek, N., Tansey, E., Goldman, B., 2018. American archives and climatic change: risks and adaptation. *Climate Risk Management* 20, 111–125.
- McDermott, F., 2004. Palaeo-climate reconstruction from stable isotope variations in speleothems: a review. *Quat. Sci. Rev.* 23, 901–918.
- McDermott, F., Atkinson, T.C., Fairchild, I.J., Baldini, L.M., Matthey, D.P., 2011. A first evaluation of the spatial gradients in $\delta^{18}\text{O}$ recorded by European Holocene speleothems. *Global Planet. Change* 79, 275–287.
- McMichael, A.J., 2012. Insights from past millennia into climatic impacts on human health and survival. *Proc. Natl. Acad. Sci. U. S. A.* 109, 4730–4737.
- Mjell, T.L., Ninnemann, U.S., Eldevik, T., Kleiven, H.K.F., 2015. Holocene multidecadal to millennial-scale variations in Iceland-Scotland overflow and their relationship to climate. *Paleoceanography* 30, 558–569.
- Mojtahid, M., Durand, M., Coste, P.-O., Toucanne, S., Howa, H., Nizou, J., Eynaud, F., Penaud, A., 2019. Millennial-scale Holocene hydrological changes in the northeast Atlantic: new insights from 'La Grande Vasière' mid-shelf mud belt. *Holocene* 29, 467–480.
- Moossen, H., Bendle, J., Seki, O., Quillmann, U., Kawamura, K., 2015. North Atlantic Holocene climate evolution recorded by high-resolution terrestrial and marine biomarker records. *Quat. Sci. Rev.* 129, 111–127.
- Oster, J.L., Warken, S.F., Sekhon, N., Arienzo, M.M., Lachniet, M., 2019. Speleothem Paleoclimatology for the Caribbean, Central America, and North America. *Quaternary* 2–5.
- Otto-Bliesner, B.L., Braconnot, P., Harrison, S.P., Lunt, D.J., Abe-Ouchi, A., Albani, S., Bartlein, P.J., Capron, E., Carlson, A.E., Dutton, A., Fischer, H., Goelzer, H., Govin, A., Haywood, A., Joos, F., LeGrande, A.N., Lipscomb, W.H., Lohmann, G., Mahowald, N., Neherbass-Ahles, C., Pausata, F.S.R., Peterschmitt, J.-Y., Phipps, S.J., Renssen, H., Zhang, Q., 2017. The PMIP4 contribution to CMIP6 – Part 2: Two interglacials, scientific objective and experimental design for Holocene and Last Interglacial simulations. *Geosci. Model Dev.* 10, 3979–4003.
- Otto-Bliesner, B.L., Tomas, R., Brady, E.C., Ammann, C., Kothavala, Z., Clauzet, G., 2006. Climate sensitivity of moderate and low-resolution versions of CCSM3 to preindustrial forcings. *J. Clim.* 19, 2567–2583.
- Peyron, O., Combourieu-Nebout, N., Brayshaw, D., Goring, S., Andrieu-Ponel, V., Desprat, S., Fletcher, W., Gambin, B., Ioakim, C., Joannin, S., Kotthoff, U., Kouli, K., Montade, V., Pross, J., Sadori, L., Magny, M., 2017. Precipitation changes in the Mediterranean basin during the Holocene from terrestrial and marine pollen records: a model–data comparison. *Clim. Past* 13, 249–265.
- Proctor, C.J., Baker, A., Barnes, W.L., 2002. A three thousand year record of North Atlantic climate. *Clim. Dynam.* 19, 449–454.
- Psomiadis, D., Dotsika, E., Albanakis, K., Ghaleb, B., Hillaire-Marcel, C., 2018. Speleothem record of climatic changes in the northern Aegean region (Greece) from the Bronze Age to the collapse of the Roman Empire. *Palaeogeogr. Palaeoclimatol. Palaeoecol.* 489, 272–283.
- Regattieri, E., Zanchetta, G., Drysdale, R., Isola, I., Hellstrom, J., Dallai, L., 2014. Lateglacial to Holocene trace element record (Ba, Mg, Sr) from corchia cave (Apuan Alps, central Italy): paleoenvironmental implications. *J. Quat. Sci.* 29, 381–392.
- Sha, L., Ait Brahim, Y., Wassenburg, J.A., Yin, J.J., Peros, M.C., Cai, Y., Li, H., Du, W., Zhang, H., Edwards, R.L., Cheng, H., 2019. How far north did the African monsoon fringe expand during the African humid period? Insights from southwest Moroccan speleothems. *Geophys. Res. Lett.* 46 <https://doi.org/10.1029/2019GL084879>.
- Sharifi, A., Pourmand, A., Canuel, E.A., Ferer-Tyler, E., Peterson, L.C., Aichner, B., Feakins, S.J., Daryae, T., Djamali, M., Beni, A.N., Lahijani, H.A.K., Swart, P.K., 2015. Abrupt climate variability since the last deglaciation based on a high-resolution, multi-proxy peat record from NW Iran: the hand that rocked the Cradle of Civilization? *Quat. Sci. Rev.* 123, 215–230.
- Smith, A.C., Wynn, P.M., Barker, P.A., Leng, M.J., Noble, S.R., Tych, W., 2016. North Atlantic forcing of moisture delivery to Europe throughout the Holocene. *Sci. Rep.* 6, 24745.
- Sundqvist, H.S., Holmgren, K., Moberg, A., Spötl, C., Mangini, A., 2010. Stable isotopes in a stalagmite from NW Sweden document environmental changes over the past 4000 years. *Boreas* 39, 77–86.
- Sundqvist, H.S., Kaufman, D.S., McKay, N.P., Balascio, N.L., Briner, J.P., Cwynar, L.C., Sejrup, H.P., Seppä, H., Subetto, D.A., Andrews, J.T., Axford, Y., Bakke, J., Birks, H. J.B., Brooks, S.J., de Vernal, A., Jennings, A.E., Ljungqvist, F.C., Rühland, K.M., Saenger, C., Smol, J.P., Viau, A.E., 2014. Arctic Holocene proxy climate database – new approaches to assessing geochronological accuracy and encoding climate variables. *Clim. Past* 10, 1605–1631.
- Thatcher, D.L., Wanmaker, A.D., Denniston, R.D., Asmerom, Y., Polyak, V.J., Fullick, D., Ummenhofer, C.C., Gillikin, D.P., Haws, J.A., 2020. Hydroclimate variability from western Iberia (Portugal) during the Holocene: insights from a composite stalagmite isotope record. *Holocene* 1–16. <https://doi.org/10.1177/0959683620908648>.
- Treble, P., Shelley, J.M.G., Chappell, J., 2003. Comparison of high resolution subannual records of trace elements in a modern (1911–1992) speleothem with instrumental climate data from southwest Australia. *Earth Planet Sci. Lett.* 216, 41–153.
- Ummenhofer, C.C., Seo, H., Kwon, Y.-O., Parfitt, R., Brands, S., Joyce, T.M., 2017. Emerging European winter precipitation pattern linked to atmospheric circulation changes over the North Atlantic region in recent decades. *Geophys. Res. Lett.* 44 <https://doi.org/10.1002/2017GL074188>.
- van Rampelebergh, M., Verheyden, S., Allan, M., Quinif, Y., Keppens, E., Claeys, P., 2014. Monitoring of a fast-growing speleothem site from the Han-sur-Lesse cave, Belgium, indicates equilibrium deposition of the seasonal $\delta^{18}\text{O}$ and $\delta^{13}\text{C}$ signals in the calcite. *Clim. Past* 10, 1871–1885.
- Warken, S.F., Fohlmeister, J., Schröder-Ritzrau, A., Constantin, S., Spötl, C., Gerdes, A., Esper, J., Frank, N., Arps, J., Terente, M., Riechelmann, D.F., Mangini, A., Scholz, D., 2018. Reconstruction of late Holocene autumn/winter precipitation variability in SW Romania from a high-resolution speleothem trace element record. *Earth Planet Sci. Lett.* 499, 122–133.
- Yeager, S.G., Shields, C.A., Large, W.G., Hack, J.J., 2006. The low-resolution CCSM3. *J. Clim.* 19, 2545–2566.
- Zanchetta, G., Drysdale, R.N., Hellstrom, J.C., Fallick, A.E., Isola, I., Gagan, M.K., Pareschi, M.T., 2007. Enhanced rainfall in the western Mediterranean during deposition of sapropel S1: stalagmite evidence from corchia cave (central Italy). *Quat. Sci. Rev.* 26, 279–286.
- Zanchetta, G., Bar-Matthews, M., Drysdale, R.N., Lionello, P., Ayalon, A., Hellstrom, J.C., Isola, I., Regattieri, E., 2014. Coeval dry events in the central and eastern

- Mediterranean basin at 5.2 and 5.6 ka recorded in Corchia (Italy) and Soreq caves (Israel) speleothems. *Global Planet. Change* 122, 130–139.
- Zanchetta, G., Regattieri, E., Isola, I., Drysdale, R.N., Bini, M., Banerji, I., Hellstrom, J. C., 2016. The so-called "4.2 event" in the central Mediterranean and its climatic teleconnections. *Alpine and Mediterranean Quaternary* 29, 5–17.
- Zhang, H., Brahim, Y.A., Li, H., Zhao, J., Kathayat, G., Tian, Y., Baker, J., Wang, J., Zhang, F., Ning, Y., Edwards, R.L., Cheng, H., 2019. The Asian summer monsoon: teleconnections and forcing mechanisms – a review from Chinese speleothem $\delta^{18}\text{O}$ records. *Quaternary* 2–26.